Equation of state and elasticity of FeSi

R. Caracas[1] and R. Wentzcovitch

Department of Chemical Engineering and Materials Science, University of Minnesota, Minneapolis, Minnesota, USA

Received 25 May 2004; revised 5 August 2004; accepted 26 August 2004; published 26 October 2004.

[1] FeSi may be one of the main products of the reaction between molten iron and mantle silicates. We use both the Local Density Approximation (LDA) and the Generalized Gradient Approximation (GGA) to Density Functional Theory (DFT) to analyze the structural behavior of FeSi and to determine its elastic properties up to high pressures. According to our calculations, at lowermost mantle pressure conditions, FeSi is in the B2 (CsCl-type) structure. The B20-B2 transition takes place at 30 GPa in LDA and 40 GPa in GGA and is characterized by a 0.35 g/cm^3 shift in density. *INDEX TERMS:* 3909 Mineral Physics: Elasticity and anelasticity; 3919 Mineral Physics: Equations of state; 3924 Mineral Physics: High-pressure behavior; 7207 Seismology: Core and mantle. **Citation:** Caracas, R., and R. Wentzcovitch (2004), Equation of state and elasticity of FeSi, *Geophys. Res. Lett.*, *31*, L20603, doi:10.1029/2004GL020601.

1. Introduction

[2] The most dramatic interface in the Earth is the core-mantle boundary (CMB). The changes in chemistry, density, viscosity, elasticity, etc. are at least as great as those occurring at the interface between the solid Earth crust and the hydrosphere. The region near the CMB surface has also played an important role in the evolution of both the core and the mantle throughout the geological time. The mantle-side part of the CMB consists of a significant chemical and thermal boundary layer, a few hundred kilometers thick, denoted as the D″ layer [*Lay et al.*, 1998]. One of the complex phenomena that are likely to occur within this layer is an influx of iron from the molten core and its subsequent reaction with the solid (Mg, Fe)SiO_3 [*Knittle and Jeanloz*, 1989, 1991; *Goarant et al.*, 1992]. This reaction, recorded experimentally above 24 GPa, generates $MgSiO_3$, MgO, FeO and FeSi.

[3] From these materials, FeSi is the least studied one. Its presence in the D″ layer may considerably affect the elasticity and the electrical conductivity of this layer.

[4] FeSi has a cubic structure at ambient conditions, B20, with $P2_13$ symmetry, where both Fe and Si atoms occupy 4a (x,x,x) Wyckhoff positions. The particularity of this structure is the seven-fold coordination for both the Fe and Si atoms. The evolution of the structural parameters was recorded experimentally up to 8.5 GPa [*Wood et al.*, 1996]. Theoretical calculations [*Moroni et al.*, 1999; *Vocadlo et al.*, 1999] showed that it transforms to a CsCl structure, B2, under pressure, above 20 GPa. Both structures are paramagnetic, the low-pressure phase semiconducting and the high-pressure one metallic. Previous ab initio calculations predicted a transition pressure of about 13–15 GPa. Measurements at high pressure [*Knittle and Williams*, 1995; *Lin et al.*, 2003a], do not report any phase transition up to 54 GPa and 2000 K, while in other experiments [*Dobson et al.*, 2002] the B2 phase was synthesized at 24 GPa and 1950 K. The B2-B20 phase transition might be enhanced by excess Fe [*Dobson et al.*, 2002; *Lin et al.*, 2003a], but further calculations and/or experiments are need to confirm it. Several other competitive structures, MnP, CoSn, NaCl, NiAs, are metastable according to ab initio calculations [*Moroni et al.*, 1999; *Vocadlo et al.*, 1999] and therefore will not be considered in the following.

[5] The compressibility of the B20 structure was determined both theoretically and experimentally. The computed values for the bulk modulus, 227 GPa (GGA results [*Vocadlo et al.*, 1999]), 257 and 209 GPa (GGA and LDA results respectively [*Moroni et al.*, 1999]), 220 GPa (LDA results [*Jarlborg*, 1995]) are larger than the experimental data. The highest recorded value is 209 GPa [*Knittle and Williams*, 1995] while all the other studies obtained smaller values: 185 GPa [*Lin et al.*, 2003a], 172 GPa [*Guyot et al.*, 1997], 160 GPa [*Wood et al.*, 1996], 115 GPa [*Zinoveva et al.*, 1974]. The B2 structure received less attention. Theoretical studies yielded for the bulk modulus values of 263 and 221 GPa (LDA and GGA, respectively [*Moroni et al.*, 1999]) and 226 GPa (GGA [*Vocadlo et al.*, 1999]), while the experimental measurements yielded 222 GPa [*Zinoveva et al.*, 1974] and 240–263 GPa (thin films of different thicknesses [*Von Kanel et al.*, 1994]).

[6] Despite the large theoretical interest and experimental effort that has recently been devoted to the study of FeSi, no report of the elasticity of this compound under pressure exists. This lead us to study the elastic constant tensor of the B20 and B2 modifications of FeSi up to 160 GPa using static first-principles calculations (T = 0K). We also determine and discuss the evolution of the structure and the equation of state of both phases.

2. Computational Details

[7] All the calculations were based on density functional theory [*Hohenberg and Kohn*, 1964; *Kohn and Sham*, 1965] as implemented in the ABINIT package [*Gonze et al.*, 2002]. ABINIT relies on the adaptation to a fixed potential of the band-by-band conjugate gradient method [*Payne et al.*, 1992] and on a potential-based conjugate-gradient algorithm for the determination of the self-consistent potential [*Gonze*, 1996]. We use the Local Density Approximation in the formulation of Perdew-Wang [*Perdew and Wang*, 1992] and the Generalized Gradient Approximation in the formulation of Perdew-Burke-Ernzerhof [*Perdew et*

[1]Now at Geophysical Laboratory, Carnegie Institution of Washington, Washington, D. C., USA.

0094-8276/04/2004GL020601$05.00

al., 1996]. The method is based on pseudopotentials and planewaves. We use Hartwigsen-Goedecker-Hutter pseudopotentials [*Hartwigsen et al.*, 1998]. In the pseudopotential construction we consider *s*, *p*, *d* and *f* projectors with 2.3, 2.4, 2.2 and 2.2 Bohr cut-off radius for Fe and 1.7, 1.9, 2.0 and 2.0 Bohr for Si (1 Bohr = 0.52917724Å).

[8] The structural relaxation was conducted using the Broyden - Fletcher - Goldfarb - Shanno minimization [*Press et al.*, 1989], modified to take into account the total energy in addition to the gradients. For the characterization of the different properties several sets of convergence tests have been carried out in order to choose correctly the grid of special k points [*Monkhorst and Pack*, 1976] and the planewave kinetic energy cut-off. The chosen planewave kinetic energy cut-off was 40 Hartree (1 Ha = 27.2116 eV). For the B20 structure we adopt a 4 × 4 × 4 grid of k points and for the B2 structure a face-centered shifted 4 × 4 × 4 grid that fold to 4 and 16 points respectively in the asymmetrical wedge of the first Brillouin zone. These parameters ensure a precision in energy better than 1 mHa and in pressure better than 1 GPa.

3. Results and Discussion

[9] The structural evolution with pressure for the two phases of FeSi obtained in both LDA and GGA is presented in Table 1. The zero-pressure results are in remarkable agreement with the experimental values. For the B20 modification, our first-principles calculations underestimate the experimental lattice constants by 2.54% in LDA and by 0.24% in GGA. The calculated Fe fractional coordinate x^{Fe}, has the same value in both LDA and GGA, while the Si fractional coordinate x^{Si} is better reproduced in GGA than LDA (experimental value: 0.8419). For the B2 modification we observe the same underestimation of the lattice parameters with respect to the experimental values: −3.01% in LDA and −0.70% in GGA. These deviations from experiment fall within the normal behavior of LDA. For this class of materials, this small negative deviation is not unusual for GGA either. This trend is also observed in the previous ab initio calculations [*Moroni et al.*, 1999; *Vocadlo et al.*, 1999], where the GGA underestimation is even more pronounced than in our case. A possible reason for these results might be the unsatisfactory description of correlation effects or of relativistic effects in Fe. However, these effects are small enough, such as their neglect still yield meaningful and useful results.

[10] Based on computed P-V relations, we fit third-order Birch-Murnagham equations of state (EOS), summarized in Table 2. We obtain results comparable to the previous theoretical ones and larger than the previous experimental data. However, the first derivative of the bulk modulus, K′, is larger than the one obtained by *Vocadlo et al.* [1999].

[11] The variation of the enthalpy of FeSi as a function of pressure shows that the transition between the B20 and the B2 structures lies near 30 GPa in LDA and near 40 GPa in GGA (Figure 1). Our theoretical results situate the transition pressure higher than the previous ab initio calculations (13–15 GPa) [*Moroni et al.*, 1999; *Vocadlo et al.*, 1999]. The discrepancy between our results and the previous theoretical ones may be assigned to the inclusion of the *s*, *p*, *d* and *f* projectors in the construction of the pseudopotentials that we use, which gives a more complete representation of the behavior at high pressure.

Table 1. Structural Evolution of FeSi Under Pressure[a]

	P(GPa)	a^{B20}	x^{Fe}	x^{Si}		
Exp.[b]	0	4.465				
Exp.[b]	12.5	4.388				
Exp.[b]	19.5	4.344				
Exp.[b]	48.9	4.226				
Exp.[c]	0	4.496	0.1359	0.8419		
Exp.[d]	0	4.488				
Exp.[e]	0	4.485				
P(GPa)	a^{B20}_{LDA}	x^{Fe}_{LDA}	x^{Si}_{LDA}	a^{B20}_{GGA}	x^{Fe}_{GGA}	x^{Si}_{GGA}
0	4.3824	0.1359	0.8407	4.4856	0.1359	0.8410
10	4.3280	0.1375	0.8415	4.4225	0.1374	0.8417
20	4.2821	0.1386	0.8420	4.3699	0.1385	0.8423
50	4.1738	0.1407	0.8429	4.2490	0.1407	0.8432
80	4.0919	0.1420	0.8435	4.1597	0.1420	0.8438
120	4.0060	0.1431	0.8441	4.0672	0.1431	0.8443
160	3.9366	0.1439	0.8445	3.9934	0.1439	0.8446
P(GPa)	a^{B2}_{LDA}	a^{B2}_{GGA}	Exp.[f]			
0	2.7076	2.7721	2.7917			
10	2.6770	2.7360				
20	2.6508	2.7058				
50	2.5890	2.6358				
80	2.5419	2.5841				
120	2.4917	2.5301				
160	2.4509	2.4865				

[a]Lattice parameters, a, in Å.
[b]*Knittle and Williams* [1995].
[c]*Wood et al.* [1996].
[d]*Guyot et al.* [1997].
[e]*Lin et al.* [2003a].
[f]*Dobson et al.* [2002].

[12] The transition is associated with a 0.35 g/cm^3 shift in density, the specific volume shift being 1 Å^3/molecule in both LDA and GGA. The high-pressure B2 phase is metallic and consequently may play an important role in the D″ layer, being part of a possible electromagnetic coupling between the core and the mantle [e.g., *Lay et al.*, 1998].

[13] Next we compute the elastic constants from stress-strain relations. We apply both positive and negative monoclinic strains on the order of maximum 1.5%. The symmetry of the chosen strain tensor allows the calculation of the whole elastic constants tensor from only two distorted structures.

[14] The values obtained in LDA are, as expected, slightly larger than in GGA (Figures 2a and 2b). The B2 structure, due its higher compaction, is slightly less compressible than the B20 structure. Despite the temperature differences, if we compare our 0K static data with the values currently attributed to the D″ layer according to PREM (Figure 2c), then both the bulk modulus, K and the shear modulus, G, are larger. For the B2 phase, the bulk modulus is about 70–100 GPa larger and the shear modulus about 170–180 GPa larger than PREM values.

[15] The shear modulus, and the tetragonal shear, $T_S = (c_{11} - c_{12})/2$, are similar, with differences at ambient pressure on the order of 21–26 GPa. These differences decrease with increasing pressure, at 120 GPa being on the order of 10–15 GPa, for both phases and both functionals. The similarity of the two shear moduli is reflected in the anisotropy ratio, defined for the cubic crystals as the ratio between the shear modulus and the tetragonal shear. For the B20 phase it decreases from 1.26 at ambient pressure to

Table 2. Summary of the Theoretical (B20 and B2 Structures) and Experimental (B20 Structure) Parameters From a Third-Order Birch-Murnagham Equation of State

B20	LDA	GGA	Exp.[a]	Exp.[b]	Exp.[c]
V (Å^3)	84.090	90.174	89.015	90.39	90.193
K (GPa)	255	221	209	172	185
K′	4.143	4.175	3.5	4.0	4.75
B2	LDA	GGA			
V (Å^3)	19.598	21.374			
K (GPa)	262	220			
K′	4.553	4.796			

[a]*Knittle and Williams* [1995].
[b]*Guyot et al.* [1997].
[c]*Lin et al.* [2003a].

1.00 at 80 GPa and down to 0.93 at 160 GPa. The B2 phase presents an opposite trend. The anisotropy ratio is 0.75 (0.60) at ambient pressure in LDA (GGA), 1.03 at 120 GPa and 1.05 at 160 GPa.

[16] We calculate next the isotropic compressional (v_p) and shear (v_s) wave velocities for a polycrystalline aggregate of FeSi:

$$v_p = \sqrt{\frac{K + \frac{4}{3}G_H}{\rho}}; v_s = \sqrt{\frac{G_H}{\rho}} \quad (1)$$

considering the Voigt-Reuss-Hill scheme for the bulk and shear moduli:

$$K = \frac{c_{11} + 2c_{12}}{3}, G_H = \frac{G_V + G_R}{2}$$

where

$$G_V = \frac{c_{11} - c_{12} + 3c_{44}}{5}, G_R = \frac{5(c_{11} - c_{12})c_{44}}{4c_{44} + 3(c_{11} - c_{12})}$$

[17] The variation of v_p and v_s is plotted in Figure 3. The LDA and GGA offer similar results. The calculated values are lower than PREM by about 1.5–2 km/s for v_p and by about 0.6–0.9 km/s for v_s.

[18] The theoretical density at 0 GPa for B20 is 6.65 in LDA and 6.21 in GGA, while for B2 it is 7.05 in LDA and 6.58 in GGA. At 135 GPa it is 8.88 in LDA and 8.56 in GGA g/cm^3 for the B20 structure and 9.17 in LDA and 8.86

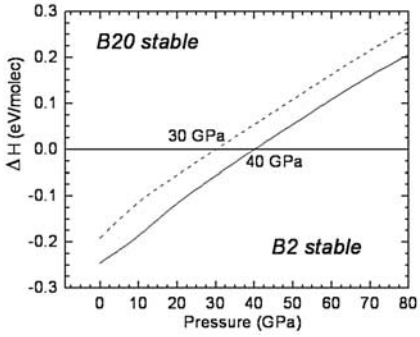

Figure 1. Enthalpy difference between the B20 and B2 structures in LDA (dashed line) and GGA (solid line).

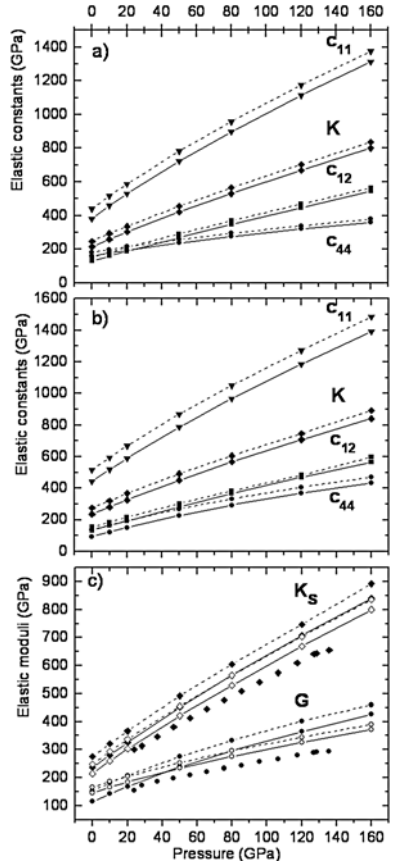

Figure 2. Pressure dependence of the elastic constants of FeSi in the B20 (a) and the B2 (b) structures, within LDA (dashed line) and GGA (solid line). K_s is the single crystal bulk modulus. c) Comparison between the isotropic polycrystalline aggregate elastic moduli for B20 (open symbols) and B2 (solid symbols) structures in LDA and GGA and PREM (symbols only).

in GGA for the B2 structure (Figure 3). Consequently, in accordance with previous experimental and theoretical results [*Dubrovisnky et al.*, 2003], FeSi is heavier than the mantle but lighter than the outer core and it may accumulate at the base of the lowermost mantle in the D″ layer.

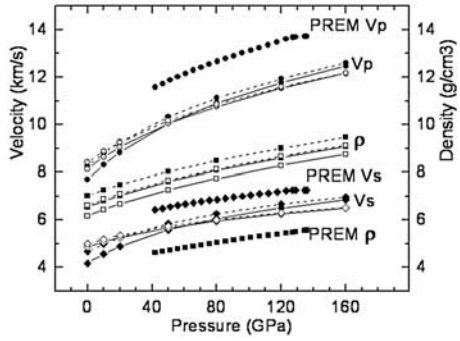

Figure 3. Densities and seismic wave velocities of B20 and B2 structures and their comparison with the PREM. Full symbols are for GGA results, while empty symbols for LDA results, continuous lines for the B2 structure and dashed lines for the B20 structure. PREM is represented by symbols only.

[19] The data that we obtained allow us to give a rough estimate about the influence of Si alloying in bcc-Fe. Thus at 0 GPa, compared to the experimental values of bcc-Fe [*Kittel*, 1976], the B2 phase has a unit cell volume smaller by about 3 and 4 $Å^3$ in LDA and GGA, respectively, and a bulk modulus larger by about 90 and 50 GPa in LDA and GGA, respectively. The shear modulus of the B2 phase of FeSi is larger by about 85 and 70 GPa in LDA and GGA respectively. With respect to bcc-$Fe_{85}Si_{15}$ [*Lin et al.*, 2003b] at about 120 GPa, FeSi is characterized by larger v_p (3–4 km/s) and v_s (2–3 km/s). Consequently, this allows us to suggest that the presence of Si in bcc-Fe should lower its density, increase its compressibility and reduce the seismic wave velocities.

[20] Our static (0 K) calculations also suggest that if present in the D″ layer, up to a few percents in volume, the B2 phase of FeSi will contribute to decrease both v_p and v_s. At high temperature, v_p and the v_s will be even smaller. The decrease is slightly more pronounced for v_p than for v_s. However, more detailed first-principles calculations, where the temperature is also taken into account are needed to clarify the effect of FeSi in the D″ layer.

[21] **Acknowledgments.** We thank A. Campbell and an anonymous reviewer for fruitful suggestions. This research was supported by the NSF grants EAR-0135533 and EAR-0230319, and the Minnesota Supercomputing Institute.

References

Dobson, D. P., L. Vocadlo, and I. G. Wood (2002), A new high-pressure phase of FeSi, *Am. Mineral.*, *87*, 784–787.

Dubrovinsky, L., et al. (2003), Iron-silica interaction at extreme conditions and the electrically conducting layer at the base of Earth's mantle, *Nature*, *422*, 58–61.

Goarant, F., F. Guyot, J. Peyronneau, and J. P. Poirier (1992), High-pressure and high-temperature reactions between silicates and liquid iron alloys, in the diamond anvil cell, studied by analytical electron microscopy, *J. Geophys. Res.*, *97*, 4477–4487.

Gonze, X. (1996), Towards a potential-based conjugate gradient algorithm for order-N self-consistent total energy calculations, *Phys. Rev. B*, *54*, 4383–4386.

Gonze, X., et al. (2002), First-principles computation of material properties: The ABINIT software project, *Comput. Mater. Sci.*, *25*, 478–492.

Guyot, F., J. Zhang, I. Martinez, J. Matas, Y. Ricard, and M. Javoy (1997), P-V-T measurements of iron silicide (epsilon-FeSi): Implications for silicate-metal interactions in the early Earth, *Eur. J. Mineral.*, *9*, 277–285.

Hartwigsen, C., S. Goedecker, and J. Hutter (1998), Relativistic separable dual-space Gaussian pseudopotentials from H to Rn, *Phys. Rev. B*, *58*, 3641–3662.

Hohenberg, P., and W. Kohn (1964), Inhomogeneous electron gas, *Phys. Rev. B*, *136*, 864–871.

Jarlborg, T. (1995), Low-temperature properties of ϵ-FeSi from ab initio band theory, *Phys. Rev. B*, *51*, 11,106–11,109.

Von Kanel, H., M. Mendik, K. A. Mader, N. Onda, S. Goncalves-Conto, C. Schwarz, G. Malegori, L. Miglio, and F. Marabelli (1994), Elastic and vibrational properties of pseudomorphic FeSi films, *Phys. Rev. B*, *50*, 3570–3576.

Kittel, C. (1976), *Introduction to Solid State Physics*, John Wiley, Hoboken, N. J.

Knittle, E., and R. Jeanloz (1989), Simulating the core-mantle boundary: An experimental study of high-pressure reactions between silicates and liquid iron, *Geophys. Res. Lett.*, *16*, 609–612.

Knittle, E., and R. Jeanloz (1991), Earth's core-mantle boundary: Results of experiments at high pressures and temperatures, *Science*, *251*, 1438–1443.

Knittle, E., and Q. Williams (1995), Static compression of ϵ-FeSi and an evaluation of reduced silicon as a deep Earth constituent, *Geophys. Res. Lett.*, *22*, 445–448.

Kohn, W., and L. J. Sham (1965), Self-consistent equations including exchange and correlation effects, *Phys. Rev. A*, *140*, 1133–1138.

Lay, T., Q. Williams, and E. J. Garnero (1998), The core-mantle boundary layer and deep Earth dynamics, *Nature*, *392*, 461–468.

Lin, J.-F., A. Campbell, D. L. Heinz, and G. Shen (2003a), Static compression of iron-silicon alloys: Implications for silicon in the Earth's core, *J. Geophys. Res.*, *108*(B1), 2045, doi:10.1029/2002JB001978.

Lin, J.-F., V. V. Struzhkin, W. Sturhahn, E. Huang, J. Zhao, M. Y. Hu, E. E. Alp, H.-k. Mao, N. Boctor, and R. J. Hemley (2003b), Sound velocities of iron-nickel and iron-silicon alloys at high pressures, *Geophys. Res. Lett.*, *30*(21), 2112, doi:10.1029/2003GL018405.

Monkhorst, H. J., and J. D. Pack (1976), Special points for Brillouin-zone integrations, *Phys. Rev. B*, *13*, 5188–5192.

Moroni, E. G., W. Wolf, J. Hafner, and R. Podloucky (1999), Cohesive, structural, and electronic properties of Fe-Si compounds, *Phys. Rev. B*, *59*, 12,860–12,871.

Payne, M. C., M. P. Teter, D. C. Allan, T. A. Arias, and J. D. Joannopoulos (1992), Iterative minimization techniques for ab initio total-energy calculations: Molecular dynamics and conjugate gradients, *Rev. Mod. Phys.*, *64*, 1045–1097.

Perdew, J. P., and Y. Wang (1992), Accurate and simple analytic representation of the electron-gas correlation energy, *Phys. Rev. B*, *45*, 13,244–13,249.

Perdew, J. P., K. Burke, and M. Ernzerhof (1996), Generalized gradient approximation made simple, *Phys. Rev. Lett.*, *77*, 3865–3868.

Press, W. H., B. P. Flannery, S. A. Teukolsky, and W. T. Vetterling (1989), *Numerical Recipes: The Art of Scientific Computing (FORTRAN Version)*, Cambridge Univ. Press, New York.

Vocadlo, L., G. D. Price, and I. G. Wood (1999), Crystal strucutre, compressibility and possible phase transitions in ϵ-FeSi studied by first-principles pseudopotential calculations, *Acta Crystallogr., Sect. B Struct. Sci.*, *55*, 484–493.

Wood, I. G., W. I. F. David, S. Hull, and G. D. Price (1996), A high-pressure study of ϵ-FeSi, between 0 and 8.5 GPa, by time-of-flight neutron powder diffraction, *J. Appl. Crystallogr.*, *29*, 215–218.

Zinoveva, G. P., L. P. Andreeva, and P. V. Geld (1974), Elastic constants and dynamics of crystal lattice in monosilicides with B20 structure, *Phys. Status Solidi A*, *23*, 711–719.

R. Caracas, Geophysical Laboratory, Carnegie Institution of Washington, 5251 Broad Branch Rd., N.W., Washington, DC 20015, USA. (r.caracas@gl.ciw.edu)

R. Wentzcovitch, Department of Chemical Engineering and Materials Science, University of Minnesota, Minneapolis, MN, USA.